

## 6.16 Integrated Proposal by the European Molecular Biology Laboratory for Beam Lines at the PETRA III Storage Ring

### 6.16.1 Introduction

**Authors:** Matthias Wilmanns, Christoph Hermes, Victor Lamzin,  
Wolfram Meyer-Klaucke, Dmitri Svergun & Paul Tucker

**Address:** EMBL c/o DESY, Notkestrasse 85, D-22603 Hamburg, Germany

#### 6.16.1.1 Summary

The European Molecular Biology Laboratory (EMBL) presents a proposal to build and operate synchrotron radiation beamlines and/or experimental stations in life sciences at the dedicated PETRA III storage ring. The document comprises detailed proposals for beamlines in Biological Macromolecular X-ray Crystallography (MX) in Biological X-ray Scattering (SAXS) and Biological X-ray Absorption Spectroscopy (XAS).

#### 6.16.1.2 Past achievements in provision of synchrotron radiation beam line facilities at the DORIS storage ring

The EMBL-Hamburg Outstation has thirty years of experience in the provision of synchrotron radiation beamlines in life sciences at the DORIS storage ring and in research activities that are associated with the experiments at these beamlines. The basis of these activities has been the provision of synchrotron radiation by the Deutsches Elektronen-Synchrotron (DESY) free of charge. The experimental end-stations including all beamline optics 'behind the beryllium window' (i.e. proximal to the end-stations) have been designed, built and are being maintained by EMBL.

While during the first two decades the amount of activities in MX, SAXS and XAS was comparable, the reconfiguration of the DORIS ring into a dedicated source and the addition of the bypass with seven wiggler stations in 1992 permitted a massive increase of experiments, particularly in MX. During the last ten years three additional MX beamlines (BW7A, BW7B, X13) were completed bringing the total number of EMBL beamlines to seven, in addition to the already existing ones (X11 and X31, MX; X33, SAXS; EXAFS; XAS). An eighth, energy-tunable beamline (X12, MX) is currently being commissioned.

The infrastructure of these beamlines is complemented by the EMBL building (25A) that has been extended by an additional floor in 2002. It hosts a molecular and biochemistry laboratory with about 40 experimental benches, a scientific library, a computer department, an administrative section and office space for about 80 staff and fellows, including some limited facilities for external users. The locally available EMBL infrastructure is integrated into the unique multiple-site structure of EMBL with its head quarters in Heidelberg (Germany) and further units in Hinxton Hall / Cambridge (UK), Grenoble (France) and Monterotondo / Rome (Italy). Various research opportunities and services from these units are directly available to the EMBL-Hamburg Outstation.

While the EMBL-Hamburg facilities were typically used by about 50-100 users per annum during the first two decades these numbers boosted during the late 90ties to 400-500 user visits per year. During these years, in MX more than 10 % of the X-ray structures of biological macromolecules world-wide that were collected using synchrotron radiation and deposited in the Protein Data Bank (PDB) originated from experiments at EMBL-Hamburg beamlines - this is the largest contribution from an European synchrotron facility. We estimate that the world-wide share of SAXS and XAS data from EMBL-Hamburg, although no systematic statistics are available, are within comparable range. More recently, the two new 3<sup>rd</sup> generation synchrotron facilities in the US (APS) and Europe (ESRF) are generally taking the lead.

At present, the EMBL-Hamburg facilities are used for about 300 external research projects per annum, of which most are from countries in Europe. While in biological MX most of the external research groups are applying for beam time at more than one synchrotron radiation facility in parallel and their projects are generally not in collaboration with EMBL-Hamburg scientific staff, most of the external SAXS and XAS experiments are in collaboration with the respective research teams at EMBL-Hamburg. In response to the flexible needs for experiments in MX, an electronic beamtime booking system was introduced in 2001 ([www.embl-hamburg.de](http://www.embl-hamburg.de)). Most of the present efforts are directed towards improvements of user friendliness, inter-operability, automation and increase of throughput at the available EMBL beamlines. Recent and present highlights are the provision of software packages for automatic data interpretation in MX and SAXS and the implementation of a robot for sample changing at one of the MX beamlines.

Core resources for the present operation of the EMBL-Hamburg beamlines come from general funding of EMBL by its member states (Austria, Belgium, Denmark, Finland, France, Germany, Greece, Ireland, Israel, Italy, The Netherlands, Norway, Portugal, Spain, Sweden, Switzerland, United Kingdom). They primarily cover the provision of required infrastructures and staff devoted to the scientific and technical support of these activities. During the last decade, access of external users was supported by schemes set up by the European Union for transnational access to infrastructures within its member and associated states. The present infrastructures have also benefited from several research project grants that have been associated with specific beamline activities. At present, the EMBL-Hamburg Outstation participates in / coordinates three major structural proteomics grants (two from the European Union, one from the German Ministry for Science and Education). For the last two years, some beamtime at the EMBL-Hamburg beamlines were used by industrial users. An academic consortium, formed by the Institute for Molecular Biotechnology (IMB) Jena, Germany, and the University of Hamburg, Germany, have substantially invested into the most recent MX beamline X13 at the DORIS storage ring.

### **6.16.1.3 Future life science oriented synchrotron radiation beamlines and experimental stations at the PETRA III storage ring**

Having the opportunity to build state-of-the-art synchrotron radiation beamlines for applications in life sciences will be central and essential for future activities of the EMBL-Hamburg Outstation. Our proposal is guided by the aims to tightly integrate the provision of com-

plementary structural biology techniques that are associated with synchrotron radiation and interdisciplinary research opportunities. The present proposal is limited to techniques that have been established in Hamburg (MX, SAXS, XAS), however, keeping options open to move into novel research methods and areas allowing the determination of structures, shapes and images of biological entities and their structural dynamics associated with biological processes. A key component of the future PETRA III beamline research activities in structural biology will be the establishment of an experimental platform to accumulate expertise and to develop novel experiments for the X-ray Free Electron Laser facility that DESY is planning to set up, exploiting its expected unique specific properties such as coherence, time structure and intensity.

The EMBL-Hamburg Outstation proposes to make use of the last two straight sections at the dedicated PETRA III storage ring (sections 8 and 9) and to build experimental stations in biological SAXS and MX (Fig. 6.16.1). For biological XAS, we propose a flexible experimental station, which may be combined with related beamline activities by HASYLAB/DESY or other research institutes. We wish to have this station at section 7, thus allowing usage of facilities shared with biological SAXS and MX. In order to make effective and synergistic use of these facilities and to promote their integration we are proposing a joint research area for life sciences. In essence, such joint facility could provide an integrated format for biological sample preparation, on-line data processing and interpretation, and common service logistics (see below). It may serve as a common platform to promote combined approaches using different and complementary structural biology techniques associated with the availability of synchrotron radiation.

### Common area for biological sample preparation

There is wide consensus that today the rate limiting step in structural biology is in the preparation of biological samples suitable for subsequent experiments using synchrotron radiation. In X-ray crystallography, in addition the availability of crystals with sufficient diffraction properties is an essential requirement. Achieving these goals becomes even more demanding when moving to large multi-component assemblies and integral membrane proteins. Common to all suggested experimental structural biology techniques, is the availability of biological samples that are homogeneously associated and can be obtained in concentrations in the mM range. Therefore, it will be essential to interface the future EMBL beamline facilities with a common area for sample preparation, characterization and crystallization.

**Sample purification:** The proposed infrastructure will provide facilities that will allow purification steps that lead to pure samples with measurable feasibility for structural biology experiments. These steps will require equipment primarily suitable for affinity and size exclusion chromatography. Any preceding steps for initial sample preparation (cloning, heterologous expression in prokaryotic and eukaryotic hosts as well as cell free expression systems, initial purification steps) are expected to be carried out elsewhere, either in laboratories of external visitors or within the existing infrastructure of the EMBL-Hamburg Outstation building 25A.

**Sample characterization:** The proposed infrastructure will provide equipment to characterize the purity and the biophysical status of biological samples by electrophoretic methods

(SDS-PAGE, native electrophoresis, isoelectric focusing), by scattering methods (dynamic light scattering), by sedimentation methods (analytic ultracentrifugation), spectroscopy methods (absorption, fluorescence emission, circular dichroism) and by the application of diagnostic tools for precise identification of probe compositions such as mass spectrometry. In addition, we are proposing to provide specific equipment for the analysis of protein-ligand interactions (proteins, DNA/RNA, lipids, other biological molecules), considering the anticipated increasing demands to provide structural biology solutions for biological complexes as opposed to single molecules. For this, we are proposing to provide equipment for isothermal micro-calorimetry measurements and plasmon resonance measurements.

**High-throughput crystallization:** It is proposed to interface the biological MX beamlines with the high-throughput crystallization facility which is currently being planned to be initially set up in a separate building that is owned by DESY (Building 3). The major components of this facility will be robotics for solution mixing and drop dispensing, storage of crystallization trays, automated visualization of experiments, interpretation and scoring. We are planning to offer this novel facility to the external user community comparable to the present offer of synchrotron radiation beamline facilities. Once the crystallization facility

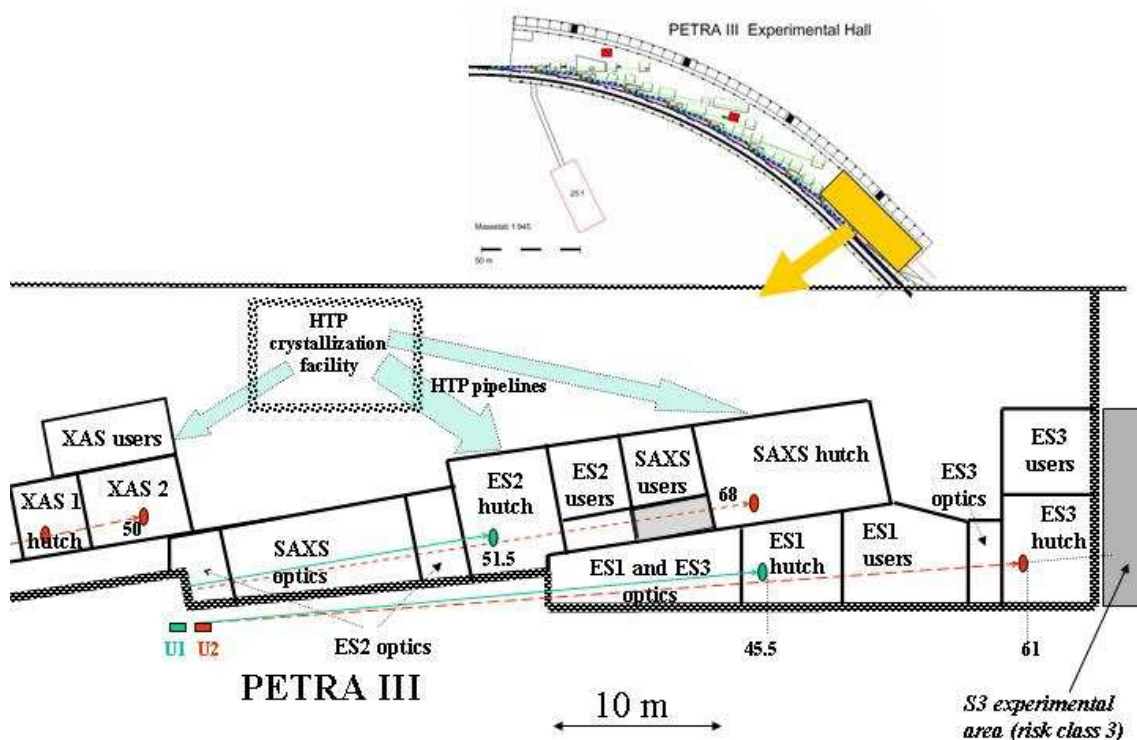


Figure 6.16.1: Schematic layout of proposed EMBL experimental stations on PETRA III.

moves into the vicinity of future PETRA III MX beamlines, we plan to establish an interface for automatic crystal transfer to those beamlines to perform test diffraction experiments as the second step of crystal 'visualization' determining their feasibility for X-ray structure determination. Given that for the presently most complex experiments in X-ray crystallography such as the ribosome or multi-component signalling complexes often thousands of crystals needed to be tested, such automated pipeline for crystal feasibility assessment may become a pivotal element in future experiments.

There will be 50 m<sup>2</sup> laboratory space available for each sample purification, sample characterization and for high-throughput crystallization.

### **On-line data acquisition, processing and interpretation**

It is anticipated that packages for the automatic interpretation of experiment data acquired at the PETRA III beamlines will be available, based on past and present developments such as ARP/wARP (MX) and ATSAS (SAXS). We propose a joint infrastructure with sufficient work space to carry out simultaneous work by ten scientists. The working area may also be used for training and teaching purposes. It will be equipped with computers suitable for graphics based data processing and interpretations and document processing. About 80 m<sup>2</sup> of office space is foreseen.

### **General services**

Although we do expect to keep most of our current central services within the present building (25A), there will be limited requirement for the provision of a computer infrastructure, safety instructions and administration. For this purpose about 50 m<sup>2</sup> of office space will be allocated.

### **Facility for sample handling and X-ray measurements at the S3 security level (future extension)**

We propose to keep an option for one of the proposed MX beamlines to make it available for biological samples requiring S3 safety level. Although the actual construction of such facility is not a part of this proposal we wish already at this stage to make an allowance for an extension of a beam pipe into an S3 containment building where diffraction experiments on pathogenic organisms could be performed under the required safety regime. For this facility about 200 m<sup>2</sup> of additional laboratory space outside of the experimental hall but close to the protein crystallography beamlines is foreseen.

#### **6.16.1.4 Support for present operation and proposal for future support**

The EMBL-Hamburg proposal for PETRA III beamlines is based on the consideration that, after an intermediate phase of parallel operation of beamlines at DORIS and PETRA III, future operation of PETRA III beamlines will be possible with a funding scheme that is

comparable to the present one. However, the design and the construction of these beamlines will require capital investments that are estimated to be in the order of 16.3 M€.

In the context of a recent application to the European Union in spring 2003, the EMBL-Hamburg Outstation has received written support from a total of 83 research institutes that are situated in Europe and Israel. These institutes constitute a large fraction of the EMBL-Hamburg user community. Given the superior parameters calculated for beamlines at the PETRA III storage ring, we anticipate that there will be even wider interest, including research groups that are not yet part of the EMBL-Hamburg user community.

Building on previous models and experience from partnerships associated with the present DORIS beamlines, the EMBL-Hamburg Outstation is also keen to establish new partnerships with academic and industrial consortia for future beamlines at the PETRA III storage ring. At present, research centers from the Helmholtz Society and Aventis Pharma have expressed interest to become putative partners. We anticipate, that once a formal proposal has been made, more opportunities for partnerships will emerge. EMBL-Hamburg will develop own activities for seeking such partnerships.

### 6.16.2 Biological macromolecular X-ray crystallography beamlines

**Authors:** Victor Lamzin, Christoph Hermes, Santhosh Panjekar, Ehmke Pohl, Alexander Popov, Andrea Schmidt, Paul Tucker, Manfred Weiss, Matthias Wilmanns

**External advisors:**

Zigniew Dauter	BNL, Upton, USA
Andrew Leslie	LMB Cambridge, UK
Sean McSweeney	ESRF, Grenoble, France
Uwe Müller	BESSY, Berlin, Germany
Gerd Rosenbaum	APS, Chicago, USA
Andrew Thompson	SOLEIL, Gif-sur-Yvette, France

#### 6.16.2.1 Present and future challenges for biological crystallography

Over the last fifty years ([Dennis & Campbell, 2003](#) further references within), biological X-ray crystallography has evolved into an advanced field of life sciences and has provided unprecedented structural insight into three-dimensional molecular information of complicated biological processes such as oxygen transport, muscle contraction, replication of genes, immune response, biological energy conversion, photosynthesis, viral assembly, protein synthesis and signal transduction. Knowledge of spatial structures has allowed to delineate the molecular origins for diseases such as cancer, autoimmune diseases and microbial infections. The performance and contribution of biological X-ray crystallography can be readily assessed by the number of new structures being deposited in the PDB, which is increasing at a nearly exponential rate. Coupled to this, the growth in a demand for synchrotron radiation beamlines for macromolecular crystallographic experiments has risen substantially both in absolute numbers and in overall proportion. More than 80 % of PDB depositions quote the use of synchrotron beamlines thus reflecting the superiority of X-ray data from synchrotron

sources (Minor, Tomchick & Otwinowski, 2000).

Our aim is to provide synchrotron radiation beam time for macromolecular crystallography (MX) at the future PETRA III storage ring to the international user community, by offering state-of-the-art beamlines both for already established technologies (small crystals requiring microfocusing, phasing requiring energy tunability) and emerging or even novel applications (time resolved studies, novel phasing methods, ultra-high resolution, remote and high-throughput operations). Clearly, the provision of such new beamline facilities at PETRA III will require developments in X-ray structure analysis methods at a comparable scale. We intend to adapt the currently used successful model of independent assessment of the scientific quality of the applications and performed experiments. As a complement to this, we aim to maintain our tradition in training and teaching that are primarily targeted towards young researchers from the community. We also anticipate that the ongoing and future advances in technology and increased throughput in structure determination will create an unprecedented demand of remote operation of the experiments (Smith, 2003). A number of important areas of biology, representing the most demanding challenges in X-ray crystallography and providing a framework for future applications at PETRA III MX beamlines, are outlined below.

**Molecular machines and large assemblies:** In recent years, crystal structures of large biological complexes have unravelled some of the most fundamental processes in biology, such as transcription (polymerase) and translation (ribosome), import and export across membranes, and the degradation machinery by the proteasome (further citations, see: Huber, 1989; Johnson & Chiu, 2002; Yonath, 2002; Saenger, Jordan & Krauss, 2002; Harrison, 2003). Some of these complexes are integrated into biological membranes, such as photosystems I and II, the light harvesting complexes, the photo reaction center and some of the complexes of the respiratory chain. At present, the largest structures, though bearing internal symmetry, are from - in part complete - viral assemblies. Some of these structures have imposed unprecedented challenges in terms of the size of available crystals, which may be low as a few microns only (Gluehmann et al., 2001; Abola et al., 2000) and unit cell dimensions, in a few cases even exceeding 1,000 Å (Stuart et al., 2002). Many of these projects have only become feasible with the recent availability of the highest brilliance beamlines at 3<sup>rd</sup> generation synchrotron sources.

**Structure based drug discovery:** Rational drug design is a process that bases the development of a drug upon the structure of its protein target (Kuhn et al., 2002). Most pharmaceutical companies and some specialized biotech companies such as Astex, Syrrx and Structural GenomiX are employing this approach for their drug discovery pipelines and have become a significant part of the synchrotron user community. A prototype example has been the work on inhibitors of the HIV protease for finding new drugs against AIDS (Wlodawer, 2002). Although most of these approaches have been focused on small, soluble protein targets, recent advances have extended them to targets of much higher complexity, such as the ribosome (Knowles et al., 2002).

**Structural Proteomics:** The availability of a rapidly increasing number of genome sequences from a wide range of organisms has revolutionized research in life sciences and has ultimately allowed to study biological processes at complete genomic (or proteomic) scale. During the last five years a number of large-scale structural proteomics initiatives has been formed (<http://www.rcsb.org/pdb/strucgen.html>). The common aim of these initiatives

is to advance parallel, high-throughput technologies in experimental structural biology and to use them for a large number of structure determinations of a proteome. While some of the early structural proteomics initiatives have been aiming for a complete knowledge of the “fold space” (Heinemann et al., 2000), more recent projects attempt to make the structures useful for unravelling the molecular basis of biological processes (Burley & Bonanno, 2002; Sali et al., 2003) and to apply them for structure-based drug discovery screening approaches (Buchanan, 2002). A novel direction in structural proteomics oriented research emerges from recent developments and applications of experimental high-throughput methods to systematically identify and to characterize protein-ligand complexes within the proteomes of living organisms (Gavin et al., 2002). Some recent attempts to utilize this novel information, initially for a systematic low resolution imaging of these protein-protein complexes (Aloy et al., 2002), have displayed its large potential for structural proteomics on protein-ligand (protein) complexes.

**Time-resolved X-ray studies and structural dynamics:** In order to use the structures of the biological macromolecules as tools to understand their functions in biology, it is essential to investigate the dynamic changes of their structures associated with these processes. Over the last two decades, an arsenal of crystallographic methods has been developed, ranging from monochromatic to polychromatic Laue applications (Hajdu et al., 2000; Moffat, 2001). These methods require high intensity and energy tunable synchrotron radiation, permitting an experiment time regime that synchronizes with the reaction kinetics associated with, and the complementary application of spectroscopy and laser techniques, triggering and terminating reactions with at precise time intervals. Proof-of-principle case studies have demonstrated that experiments addressing specific biological questions are feasible in the nsec and even psec regime (Schotte et al., 2003; Bourgeois et al., 2003; Adachi et al., 2003). The expected time structure and optical properties of the PETRA III beamlines will provide ideal opportunities and an experimental set-up for future applications. As a spin-off, there could be also the possibility to use a pink beam option, also known as the narrow band-pass Laue data collection technique, for ultra-fast data collection. Such techniques may allow rapid exposure times in the range of  $10^{-4}$  to  $10^{-5}$  sec per frame, an improved signal-to-noise ratio, the absence of harmonic overlaps and reduced radiation damage effects. Ultimately, time resolved experiments at PETRA III could provide a basis to acquire sufficient expertise to plan and to design novel time-resolved experiments on single particles (Neutze et al., 2000) for the planned X-ray Free Electron Laser facility at DESY campus ([tesla.desy.de](http://tesla.desy.de)).

**Biological structures at atomic and sub-atomic resolution:** The number of X-ray crystal structures at atomic resolution (allowing visualization of atoms) and ultra-high resolution (visualization of electronic features), currently available from the PDB, is steadily increasing (Schmidt & Lamzin, 2002). A protein structure determined to such resolution offers a unique and extremely valuable tool by essentially closing the gap between biology and chemistry via establishing structure-function relationships in unprecedented detail in terms of accurate location of atoms (including hydrogen atoms), accurate inter-atomic distances as well as providing valuable information on the mobility and flexibility of the protein molecule even in the crystal lattice (Dauter, Lamzin & Wilson, 1997; Harata & Kanai, 2002). At ultra-high resolution, as demonstrated for crambin as a proof-of-principle case (Jelsch et al., 2000),

even atomic detail of bonding electrons and free electron pairs can be obtained. Some of the specific properties of the PETRA III ring, such as the delivery of X-rays at high energies (defining the maximum reachable resolution) and high intensity will be ideally suited for future developments and applications of atomic resolution methods for a broad variety of crystallized biological macromolecules.

**Experimental structure determination methods:** Since in MX there is an inherent need to obtain the phase component for structure determination, techniques are required to derive this information experimentally. A major source of such information can be derived from the anomalous and the dispersive signals at energies close to the absorption edge of specific elements built into the structures of biological macromolecules. While traditionally, 'heavy atoms' were used by soaking or co-crystallization, more recently the arsenal has been extended by the routine incorporation of heavy-atom substituted amino acids (selenomethionine), heavy-atom derivatised DNA and RNA (iodine, bromine), soaking with halides (Dauter & Dauter, 2001) and even the exploitation of the anomalous signals of 'light' atoms such as sulphur and phosphorus that are generally found in biological macromolecules (Micossi, Hunter & Leonard, 2002; Ramagopal, Dauter & Dauter, 2003; Uson et al., 2003). The use of a wide energy spectrum in the range of 5 - 35 keV, which can be offered by PETRA III, will provide an unique opportunity, to offer an experimental setup for a broad range of established phasing methods and to develop novel techniques, particularly aiming for exploiting the anomalous signal properties of atoms that compose biological macromolecules.

### 6.16.2.2 Instrumental considerations for X-ray stations

#### General aims

The specifications of the planned MX beamlines at PETRA III will be largely governed by the challenges emerging from the research directions presented above. Biological crystallographic experiments require an intense and very stable X-ray beam tunable in energy with small, adjustable focus and low divergence. The end-stations will be automated to a level that minimizes (and eliminates wherever possible) the need for user intervention. The X-ray beam has to be conditioned by various sets of slits and attenuators and observed by a series of viewers and beam position monitors. Our aim is to provide adequate facilities that can cope with the most demanding requirements:

- State-of-the-art tunability in terms of a broad energy range, energy band pass and excellent beam stability to provide opportunities for carrying out a variety of experimental phasing methods that are available, under development or planned.
- High brilliance coupled with small focus size to allow measurements on extremely small crystals (in the range of a few  $\mu\text{m}$ ), structures of large biological assemblies (up to the MDa range) and crystals with long unit cell dimensions ( $> 1000 \text{ \AA}$ ).
- A high degree of automation, user-friendliness and parallelism that will allow high-throughput structure determination, notably in the fields of structural proteomics and drug-discovery oriented structural biology.

- To provide the experimental conditions for measurements and structure determination at extremely high resolution ( $< 1 \text{ \AA}$ ).
- An experimental environment to allow time-resolved measurements matched to the time structure of the PETRA III ring with the intention of revealing the dynamics of biological processes.
- To allow adaptations in order to meet specific demands (lighting, data collection temperature, use of lasers, etc.).

### Specific requirements

The instrumentation requirements are outlined as follows:

1. **Beam divergence.** The divergence of the beam has to be smaller than 0.5 mrad to resolve the diffraction spots of crystals with unit cell dimensions of up to 1,000  $\text{\AA}$ .
2. **Beam size.** In order to provide the best signal-to-noise ratio in the diffraction pattern, the beam focal size has to be adjustable and made consistent with the specimen size (from 0.3 mm down to 0.02 mm).
3. **Intensity.** The X-ray intensity delivered to a sample will be about  $10^{13}$  ph/sec. Such intensity will allow collection of data from a typical protein crystal with an exposure time of about 0.1 sec per frame ( $0.5^\circ$  of oscillation). With sufficiently fast detectors (readout time of about 0.1 sec), appropriate goniometers (rotation speed of about 100-200° per second) and fast beam shutters the total data collection from a crystalline sample will take only minutes.
4. **Energy range.** Experiments utilizing anomalous dispersion properties require X-rays tunable in energy range from 5 to 35 keV (2.5 to 0.36  $\text{\AA}$ ). The higher energy limit is set by the Xe K edge; the lower energy limit is defined by transition-metal K edges and will also allow recording considerably improved anomalous signals from sulphur and phosphorus atoms.
5. **Energy resolution.** The incident spectral band pass  $\Delta E/E$  will be less than  $2 \times 10^{-4}$  to resolve specific features in absorption spectra.
6. **Beam stability.** The relative position of sample and X-ray beam must be kept constant to within 5% of the beam size or sample size (whichever is smaller).

### Instrumental design

Tab. 2.2.2 recalls the principal beam characteristics of PETRA III undulators. Very small photon source sizes, low divergence and extremely high brilliance (Fig. 2.2.2) will be ideally suited for the tasks of biological crystallography.

### 6.16.2.3 Proposed end-stations and optics

#### Overall scheme

In view of the increasing demand for structural information several important factors will be taken into consideration. Firstly, recent improvements in methodologies have provided non-specialists with the ability to carry out macromolecular structure determination. Secondly, the application of high-throughput technologies for protein production and crystallization will have a direct follow up in terms of the number of structures to be determined. Thirdly, industrial research in medicine, pharmacology, food and agriculture is poised to reap the benefits of the high throughput technologies.

To cope with the anticipated categories of experiments and with the diversity of the future user community we propose the construction of three MX beamlines. These beamlines will be in conjunction with one biological SAXS beamline (see Chapter 6.16.3) and are proposed to be situated on the last two high- $\beta$  straight sections (section 8 and section 9<sup>4</sup>) using two 2 m long undulator sources (U1 and U2) per section (Fig. 6.16.2). The SAXS station will utilize the beam from undulator U2 of the second last straight section (section 8), while the three MX stations will use U1 from the same section and both U1 and U2 undulators from the last straight section. The initial 5 mrad horizontal separation of the U1 and U2 undulator beams (i.e. 170 mm in horizontal direction at 33 m distance from the undulator) will be increased to 300 mm in the vertical direction using vertically deflecting double crystal monochromators. Thus the beam centers at the location of the downstream optics hutches and experimental stations will be separated by more than 350 mm. This vertical separation will be sufficient to permit simultaneous operation of all four experimental stations and will allow the installation of a large area detector and other bulky end-station equipment.

#### X-ray optics

The objective of the optical set-up is to deliver a monochromatic beam at a fixed position of the sample with easily and quickly adjustable X-ray energy and maximized photon flux. Ideally, both focal spot size and beam divergence will be adjustable to meet the requirements of each individual experiment.

Tab. 6.16.1 summarizes the principal characteristics of the proposed beamlines. The optics of all MX beamlines will be designed to be similar, thus allowing standardization of components design and know-how transfer, particularly during the commissioning stage. The main optical elements are liquid nitrogen cooled double-crystal monochromators and Kirkpatrick-Baez (KB) mirrors, which will be used as focusing elements and high-energy filters. The KB arrangement with two individual mirrors allows independent and tunable focusing in both the vertical and the horizontal directions.

In order to estimate the beam size, divergence, band pass and flux on the sample, ray-tracing calculations were performed using the programs XOP and SHADOW with the input parameters described in Appendix A.1.1. Some examples of these calculations are given below for the station ES3.

<sup>4</sup>These are the two last sections close to building 48, see also Fig. 2.2.1.

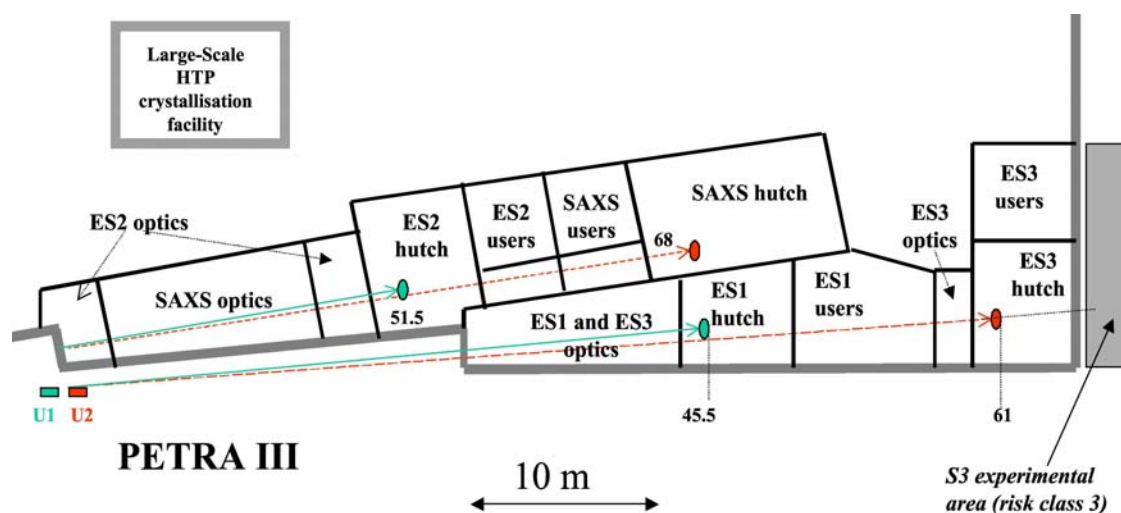


Figure 6.16.2: A schematic floor plan of the PETRA III experimental hall showing the proposed layout of the EMBL MX and SAXS beamlines.

Beamline	ES1	ES2	ES3
Main purpose	Wide range tunability	High-throughput structure production	Microfocus and special application
Energy range, keV	5.0 – 35.0	6.0 – 16.5	6.0 – 18.0
Bandpass (after monochr.) $\Delta E/E$	Si(111): $1.4 - 2.3 \cdot 10^{-4}$ Si(311): $4 - 9 \cdot 10^{-5}$	Si(111): $< 1.6 \cdot 10^{-4}$	Si(111): $< 1.7 \cdot 10^{-4}$
Min. focus size, $\mu\text{m}^2$ (horizontal x vertical)	25 x 6	24 x 6	14 x 4
Divergence of the focused beam, $\text{mrad}^2$ (horizontal x vertical)	0.3 x 0.2	0.3 x 0.2	0.5 x 0.25
Intensity, ph/sec	$3 \cdot 10^{13} - 1 \cdot 10^{12}$	$2 \cdot 10^{13}$	$2 \cdot 10^{13}$
Pink beam option, ( $\Delta E/E = 1.5 \cdot 10^{-2}$ ) Intensity, ph/sec	Possible $\sim 10^{15}$	No	No

Table 6.16.1: Parameters of planned MX beamlines / end-stations on PETRA III.

### Beamline control

The degree of automation controlling the alignment of optical components of a beamline has to be as high as possible with the final aim of a fully self-aligning system. To achieve this goal

a sufficient number of monitors distributed along the beam path is a necessary pre-requisite. As a minimum requirement these monitors will be located before and after individual optical components and provide the shape as well as intensity information. They could be based on PIN diodes and fluorescence screens and TV-cameras with frame grabbers. A robust and fast bus system for the various analog and digital signals coming from these monitors and from the encoders of various motor axes will be linked to a dedicated control computer. If not fully automatic in the first instance, the control program must enable the inexperienced user to adjust the beamline for his specific requirements.

### MX station 1 – wide range of tunability

ES1 will use the U1 undulator of the last straight section (section 9), Fig. 6.16.2. Fig. 6.16.3 shows the proposed layout of the station components.

The most important parameters for this end-station are the wavelength range (5-35 keV) and the narrow band pass ( $\Delta E/E \sim 2 \cdot 10^{-4}$ ) over the whole wavelength range. The focus does not have to be exceptionally small - about 200  $\mu\text{m}$  seem appropriate - although there will be a possibility to achieve a focus size of the order of tens of microns (Tab. 6.16.1). The specific requirements for the detector are good DQE over the entire energy range and a sufficient size to cope with the larger scattering angles at both lower X-ray energies and in high-resolution measurements.

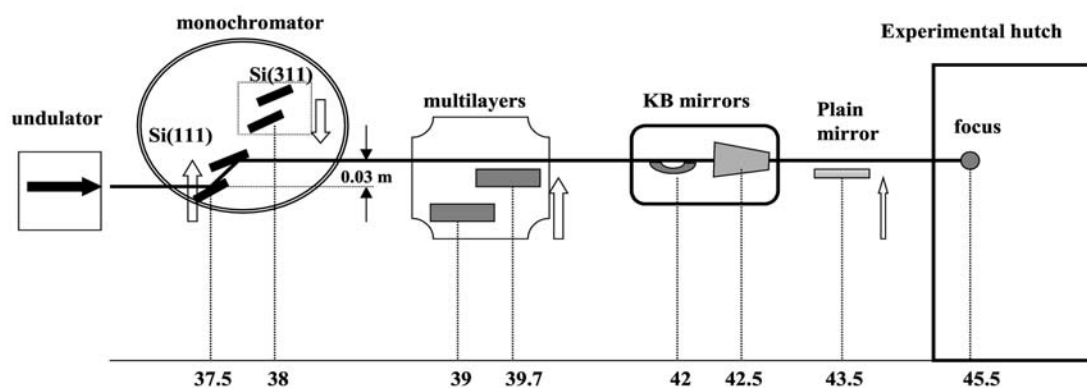


Figure 6.16.3: Layout of the optical components for ES1.

The first optical element is the fixed exit double crystal monochromator. It will be situated 37.5 m from the source point. Two monochromator crystals will be available, a high resolution Si (311) and a lower resolution Si (111). The former will be used for precise white line measurements and the latter for the softer X-ray region (below 10 keV). The Si (111) monochromator will also be used for routine measurements where high intensity is more important than energy resolution.

For high flux studies with “pink beam”, the crystal-monochromator would be replaced by a cryogenically cooled double multilayer monochromator. Due to the small incidence angle of

multilayers, the available energy range in ‘pink beam’ mode will be 8 to 13 keV.

A pair of elliptically bent mirrors in the KB configuration will be used for harmonics rejection and focusing. The first mirror positioned at 42 m from the source will provide focusing in the vertical direction (1:12 demagnification). The second mirror will reduce the horizontal beam size (1:14 demagnification). The rather broad X-ray energy range makes it necessary to coat each mirror with two different metal stripes, rhodium and platinum. Rhodium coating will be used in the energy region between 5 to 18.5 keV at a fixed incident angle of  $0.2^\circ$ . In order to provide harmonic rejection at energies below 8 keV, we propose to use an additional plain silicone mirror positioned at 2 m from the focus. The platinum coated mirror will be used at a fixed incident angle of  $0.15^\circ$  in the energy region from 18.5 to 30 keV and at a fixed incident angle of  $0.10^\circ$  in the region from 30 to 35 keV.

The focal spot size will be variable in both directions (from 25 to  $300\ \mu\text{m}$  horizontally and from 6 to  $300\ \mu\text{m}$  vertically). In order to achieve this, the image of the source provided by each individual mirror must be adjustable.

To our knowledge, ES1 would be the first MX-station to allow high-energy resolution MAD (SAD) experiments with very high intensity over such a wide range of X-ray wavelengths and at the same time serving as reliable high-energy beam line for ultra-high resolution crystallography.

### MX station 2 - high throughput structure production

ES2 is intended for high throughput structure production. It will use undulator U1 from the straight section 8 and will be located near to the Large-Scale crystallization facility, Fig. 6.16.2. Fig. 6.16.4 shows the proposed layout of the optical components. The fixed exit Si (111) double crystal monochromator will lift the beam in vertical direction by 300 mm to separate the beams from undulators U1 and U2. The large distance between the monochromator crystals will restrict the available energy range to an upper limit of 16.5 keV ( $0.75\ \text{\AA}$ ) but maintaining a certain degree of tunability over the common absorption edges is required to allow high throughput SAD or MAD experiments.

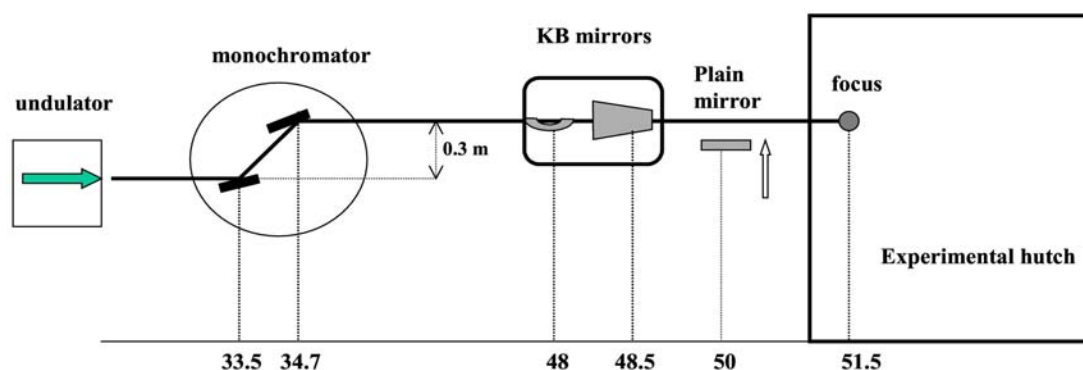


Figure 6.16.4: Layout of the optical components for ES2.

Over the last two years 80 % of the experiments at EMBL beamlines requiring tunability exploited the anomalous signals from selenium, mercury, bromine, platinum and iron. Therefore the station will be tunable over the range 6 to 16.5 keV (encompassing most absorption edges of these elements) with a band pass of  $2 \cdot 10^{-4}$  and adjustable focus. Focal spot size will be variable from 24 to 300  $\mu\text{m}$  in the horizontal direction and from 6 to 300  $\mu\text{m}$  vertically.

Both KB mirrors will have rhodium coating. In the energy range from 6 to 8.5 keV an additional plain mirror either made from Si or  $\text{SiO}_2$  or coated with a low-Z material like aluminum will be used for harmonic rejection. The first KB mirror positioned at 48 m will provide focusing in the vertical direction (1:14 demagnification), the second mirror will focus in the horizontal direction (1:16 demagnification). The mirrors will work at a fixed incident angle ( $0.2^\circ$ ).

A large and fast area detector and state-of-the-art systems for sample mounting and centering as well as automatic data evaluation are indispensable features for the end station of this beam line.

The end-station will be close to the high-throughput crystallization facility being established at the EMBL-Hamburg Outstation. In addition to the "standard" mounting-type experiments we are planning to develop a protocol for direct X-ray scanning of the free interface diffusion plates or even standard vapor diffusion plates to characterize the diffraction properties of the crystals in the trays directly. This option will be combined with the use of the microfocused beam described below.

### MX station 3 - microfocus applications

This station will use undulator U2 from the last straight section (section 9), Fig. 6.16.2. The proposed layout for ES3 is shown in Fig. 6.16.5, some of the result of ray tracing in Fig. 6.16.6. The end-station will cover the photon energy range from 6 to 18 keV with the focus size smaller than 15  $\mu\text{m}$  and a divergence of 0.5 mrad in the horizontal direction at the position of the protein crystal.

A fixed exit Si (111) double crystal monochromator will lower the beam in vertical direction by 300 mm to separate the beams from undulators U1 and U2. A plain silicone mirror positioned at 1 m distance from the focus will be used for the harmonic rejection in the energy range of 6 to 8.5 keV. Both KB mirrors will have rhodium coating and will work at a fixed incident angle ( $0.2^\circ$ ). The first KB mirror positioned at 58.5 m will provide focusing in the vertical direction (1:23.5 demagnification), the second mirror will focus in the horizontal direction (1:30 demagnification). In special cases, focusing to  $1 \times 1 \mu\text{m}^2$  or smaller will be achieved by the addition of refractive lenses after the KB mirrors.

Given the downward trend in crystal size, reflecting the increasing sizes and complexities of the samples investigated, and the frequency with which initial crystallization conditions yield very small crystals, means of characterization will become critical to determine if the crystallization conditions warrant optimization. Large plate-like crystals susceptible to radiation damage can be exposed in different places to allow complete data sets to be collected, as demonstrated, for instance, for the nucleosome core particle (Luger et al., 1997). In addition, diffraction properties often vary as a function of the way a particular part of the crystal

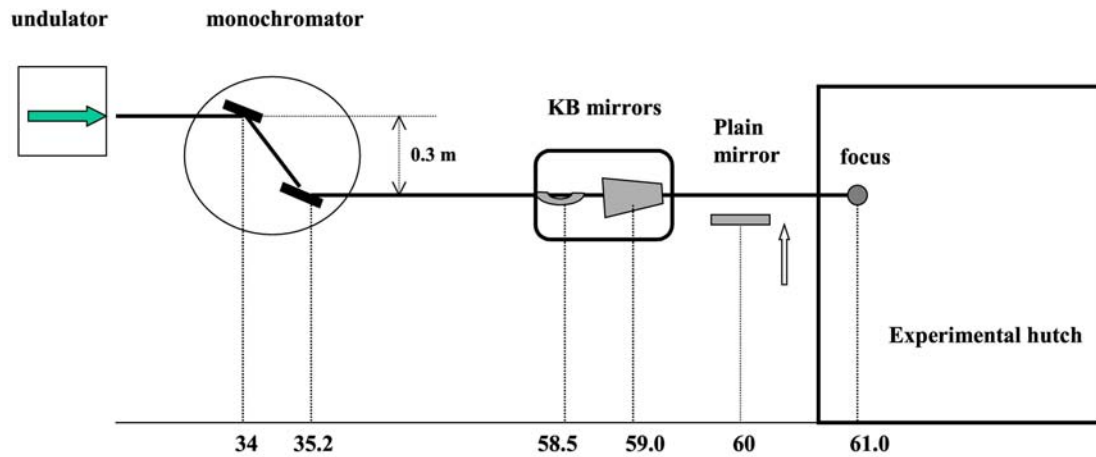


Figure 6.16.5: Layout of the optical components for ES3.

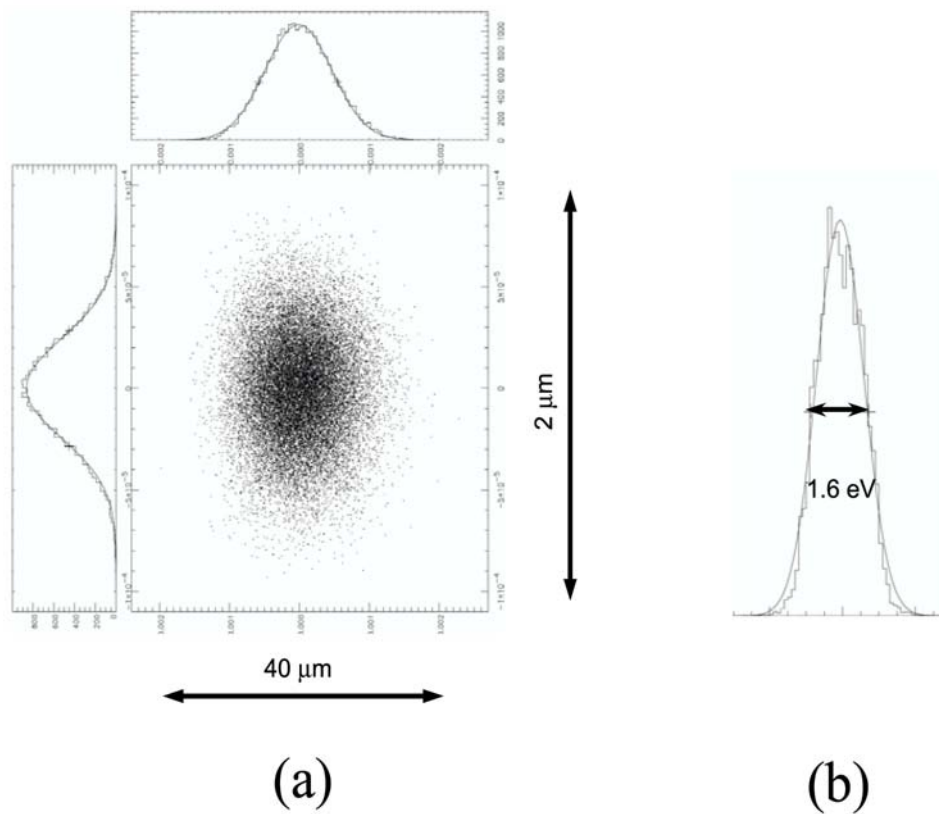


Figure 6.16.6: Ray tracing for the station ES3: (a) spatial distribution of the beam at the focal point and (b) the energy resolution as simulated by SHADOW at an energy of 12 keV.

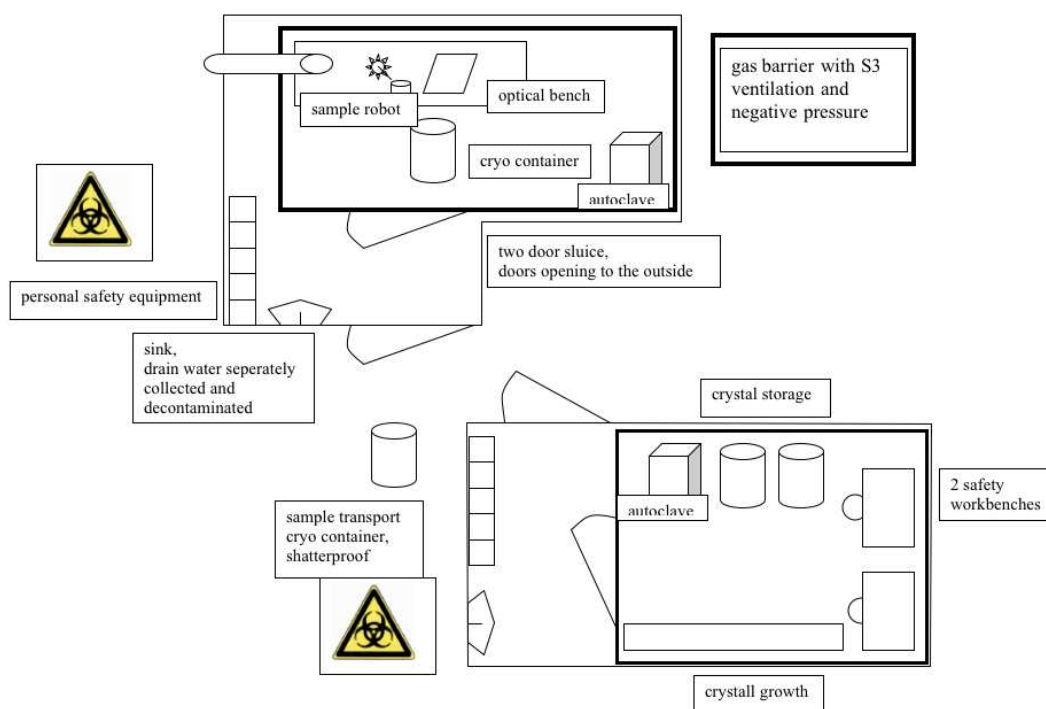


Figure 6.16.7: Layout of the future S3 X-ray facility.

has grown. The beamline ES3 will allow to screen different parts of the crystal allowing focused measurements of the “best” part that may be single or may diffract to the highest resolution.

A key feature of this end-station will be a micro-goniometer with advanced optics and a very small sphere of confusion for the rotation axis. Many of the concepts being used for the micro-goniometer at the ESRF ([www.esrf.fr](http://www.esrf.fr), [www.embl-grenoble.fr](http://www.embl-grenoble.fr)) could be adapted. Given the small volumes of the diffracting material the most important parameter for the choice of the detector will be the sensitivity.

### MX station 3 - future expansion

Given the above listed specifications for ES3 it would be the obvious choice for measuring “difficult” crystals. A further option is then to expand into a field for which currently no facility exists. Handling of certain viruses, prions and other hazardous compounds underlies strict safety rules, ranging at the level of S3. This imposes certain restrictions on the end-station construction, as it has to be ensured that the entire experimental hutch is well separated from the surroundings and can be chemically and biologically decontaminated. Also, it will be directly linked to an S3 lab for sample preparation and handling. A schematic layout of the S3 facility for applications in biological crystallography is shown in Fig. 6.16.7.

Although actual construction of an S3 facility is not a part of this proposal, allowance will be made already at this stage for the beamline ES3 to have a beam pipe, which could exit

the planned experimental hall and lead to an S3 containment building where diffraction experiments on pathogenic organisms could be performed under the required safety regime. It seems essential to offer the users an opportunity to access a facility that would allow handling and measurements of samples at an S3 safety level. Topics and potential applications that currently are of high scientific interest include the following: *prions* causing bovine spongiform encephalopathy (BSE); human Creutzfeld-Jakob disease (CJD), kuru; *retroviruses* human immunodeficiency virus (HIV), T-cell leukemia virus (HTLV) and *hepatitis viruses* A to E.

#### 6.16.2.4 End-station design: specifications for the basic end-station

EMBL will implement a novel design of the crystallographic end-stations where one basic model can be extended to the particular technical demands of each beamline. A number of technical specifications will be similar on all beamlines. Accessory equipment (e.g. a laser for experiments in time resolved crystallography or a high-pressure cell for high-energy applications) can be added when necessary. The end-stations will be designed to operate in a fully automated manner with a possibility of remote control.

#### Fast Shutter

Due to the high photon flux of the synchrotron radiation extremely short exposure times per frame can be anticipated. Given the prospect of pixel detectors with read-out times in the range of milliseconds that are currently being developed at various laboratories it is considered that diffraction data can be collected in a continuous rotation mode or with very fine slices (less than  $0.1^\circ$ ). This requires an extremely fast and accurate shutter-system that is able to close and open the X-ray beam within less than 1 msec.

#### Microfocusing and collimation

An accurate slit system is required to match the beam size optimally to the crystal size. The ES3 station will be specifically designed for applications with very small crystals down to  $5\ \mu\text{m}$  or even smaller. The accuracy of the slits system thus has to be better than  $1\ \mu\text{m}$ . Commercially available systems can already provide the required accuracy.

#### Beam viewer

A beam viewing system is an integral part of modern end-stations, e.g. the micro-goniometer at the ESRF, as mentioned above. In order to ensure that the synchrotron beam actually hits the sample at a required position, a high-accuracy beam viewing system is required. This can be accomplished by a single crystal scintillator or by a small CCD camera that is moved into the beam in order to determine the center of the beam experimentally. Should the beam be misaligned, an automatic feedback system to the optical instrument (i.e. the final mirror) will move it into the desired position. Alternatively, the entire setup could be placed on an optical bench that is positioned into the beam.

### **Visible and fluorescence light coupled to a high-resolution video microscope**

In order to identify single crystals of biological macromolecules frozen in a cryo-loop there is a need for image recognition in visual light and, possibly, in UV ranges. The idea of utilizing the inherent UV fluorescence of biological macromolecules has been originally suggested by G. Rosenbaum (Rosenbaum, unpublished) and research exploring the feasibility is currently underway at the EMBL-Hamburg Outstation and elsewhere. Whereas two images taken at 0 and 90 degrees will be sufficient to center the crystal a series could be used for shape determination. The precise determination of the shape of the sample could then be used for various applications including an empirical absorption correction for long-wavelength data collection.

### **Phi-goniostat and kappa goniometer**

The end-stations will be equipped with a fast and accurate direct drive phi-goniostat that would also allow the collection of continuous rotation data. Due to the small beam aperture and crystal size the accuracy of the crystal position as well as the sphere of confusion has to be within 5  $\mu\text{m}$  for the standard operation and within 1  $\mu\text{m}$  for the microfocus ES3 beamline. The rotation speed required is 360° per second or even faster.

The end-station ES1 will be equipped with a kappa-axis goniostat, which will allow exact crystal alignment and re-orientation for completion of blind regions in high-resolution data collection. It will be particularly useful in a critical phasing experiment or for semi-empirical absorption correction using psi-scans. The specification for the accuracy will be slightly lower for a kappa goniometer with sphere of confusion of 5  $\mu\text{m}$ .

### **Motorized beamstop**

Motorization of a beamstop is an integral component of the overall automation of the end-station. A versatile beamstop with an integrated X-ray sensor developed at SSRL has proved reliable for a variety of applications including the rapid alignment, exposure control, examination of the direct beam profile, characterization of the shutter timing and energy calibration (Ellis, Cohen & Soltis, 2003).

### **Robotic sample mounting**

A high degree of automation including robotic sample mounting is mandatory. Full software control is needed not merely to accelerate the mounting process as such, but to provide robustness in sample handling and screening and to allow complete remote control of the experiment. The vast majority of the samples will be frozen in cryo-loops on standard magnetic caps in plastic vials and supplied in standard sample containers. A sufficient-size storage container for several sample pucks will be installed at each end-station. We anticipate that by the time of the construction of the PETRA III beamlines the sample container and shipping systems will be standardized

### Detector gantry

Given the fast rate of the development of X-ray detectors it is not clear which type of detector will be available by the time of construction of the beamlines at PETRA III (see Tab. A.1.2 for the current anticipations). Therefore, we will stick to a framework that will be able to account for spatial demands and accommodate very large and heavy detectors (optionally even two different detectors). A sufficiently wide range of the sample-to-detector distance will be made available. In order to decrease air scattering at longer wavelengths an option of a helium cone covering the space between the crystal and the detector will be allowed.

#### 6.16.2.5 End-station area

##### Beamline operators

Each MX beamline will contain sufficient space for the beamline operators and provides easy access to electrical connections, computers for motor controls, monitors for temperature of optical elements, vacuum and beam position. Ideally this area will be close to the beamlines optical hutch and will be enclosed (4 to 6 m<sup>2</sup> is the minimum). Regular beamlines users will not have access to this area.

##### User area

The user area for each beamline will be quiet (and therefore insulated from the main experimental hall), will provide the necessary control, processing and graphics computers (the future is likely to see the majority of structures being processed and solved “on-site”) and will be in close proximity to the experimental hutch. Local experience at DORIS and at other synchrotron facilities will suggest an area of no less than 4x5 m<sup>2</sup> for each of the three user control areas. Given the likely shortage of space one could think of placing these user areas on top of the respective end-stations.

Indispensable components of the user area are: event-monitors for crystal, cryo-system, spindle axis, detector distance, slits, ring current, ion chamber readings, sample changer, fluorescence detector, table alignment and space for the overall set-up, desks for up to four scientists, wardrobe, safe, computers for: monitoring beamline and end-station status, data collection, data processing, computer graphics, PC for word processing and data backup facilities.

##### Sample storage facility

In order to meet the demand which is likely to arise from the “crystal in the mail”-type data collection, a facility will be installed in close proximity to the experimental hutches, in which samples received from users and ready to be mounted on the end-station, will be stored at liquid nitrogen temperature until they are scheduled for X-ray measurements. Such a storage

facility will be adapted to the to be agreed standards with respect to shipping containers, carousels and mounting robots.

The facility will include the following components:

- entry gate,
- barcode reader for sample tracking,
- robotic arm to receive and store the samples,
- storage space under liquid nitrogen temperature,
- automated nitrogen refill through a turbulence-free system,
- computer and data base for sample tracking,
- exit gate.

The facility will need to be accessible from both the outside (entry gate) and the inside of the hutch (exit gate). For practical and space reasons some elements of the manual transfer between the facility and the end-station hutches will have to be accounted for. A room of the size of minimum  $2 \times 3 \text{ m}^2$  will be sufficient. Efficient ventilation must be insured to cope with the use of large amounts of liquid nitrogen.

### **Sample preparation laboratory**

A single laboratory area no less than  $20 \text{ m}^2$ , equipped with benches, balance, fridge, deionised water, simple chemicals and basic tools for crystal handling, as well as room and tools for crystal mounting (individually or into carousels), will be in the vicinity. An additional area of  $10$  to  $20 \text{ m}^2$  or a separate enclosure for working with gases (for example for pressure derivatization of crystals with xenon or krypton), including a fume hood for derivatization with possibly toxic chemicals with a high vapor pressure and handling of heavy atom compounds (including waste containers) will also be close by. This enclosure must be ventilated to the outside and must therefore be at the edge of the experimental hall. It will also be possible to temporarily store crystallization plates in this room, which makes air conditioning / temperature stabilization necessary. Liquid nitrogen supply and equipment for cryo-freezing of crystals are absolute requirements and a dewar for storage of crystals at  $100 \text{ K}$  must be available.

### **Large-scale crystallization facility**

The large-scale crystallization facility will be installed in the vicinity of the beamline ES2, Fig. 6.16.2. It will comprise a fully automated facility involving robotics preparation of solution cocktails for crystallization, drop dispensing, plate sealer, bar-code readers, transport system to and from storage cabinets, optical crystal visualization system and supporting computer environment for full sample tracking. The facility is planned to be installed by

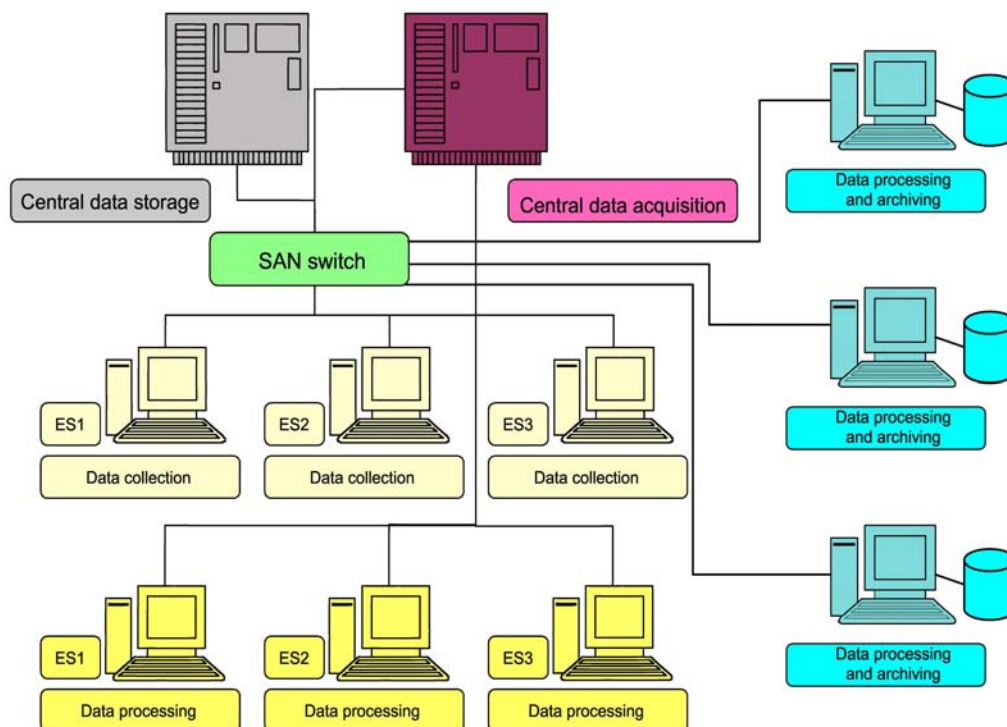


Figure 6.16.8: Schematic representation of the planned computing infrastructure for MX.

EMBL on a DESY side in 2004 and will be moved into the PETRA III hall in 2008. The minimum space requirements are of an order of  $7 \times 8 \text{ m}^2$ .

### Computer environment

For data collection and processing each beamline will be equipped with three computers, one for data collection, one for data processing and one graphics machine, Fig. 6.16.8. The data collection machine together with the central storage and data processing unit will form a storage area network (SAN) via fiber channel, where central storage device is connected via multiplexed FC uplinks. This will allow the fastest possible data transmission and will be completely independent from the normal network traffic.

The planned data storage unit can be an intelligent fiber channel RAID running RAID level 5 plus hot spare disks and a snapshot functionality so that a normal tape backup will no longer be needed. The needed capacity of the central storage device is related to the image size and the read-out speed of the detectors. The capacity will be high enough to keep data files for at least 10 days, so that users can verify that the data were successfully archived. For data archiving a fiber channel compatible tape device (LTO, SuperDLT) can be connected to the SAN switch, which will then be available from all machines in the SAN. Another possibility for data archiving is the transfer to user laptops via normal network connection.

Data processing machines are basically terminals connected to the central data processing unit via normal network connection. The central unit will consist of a cluster of machines, which can be upscaled and extended when needed.

In MX, data processing and archiving frequently still extends beyond the allocated experimental time. A major reason is within the large time-requirements, and with the small control stations advocated above, the parallel handling of two sets of experiments in this area becomes impossible. Therefore a second area containing the necessary computing and archiving facilities will also be available and common for all crystallographic end-stations. This could be placed almost anywhere in the experimental hall and will have minimum dimensions of  $3 \times 10 \text{ m}^2$ . This area will be equipped with at least three computers connected to the SAN so that fast data transfer to those machines is ensured. They will also be connected to archiving devices. For the type of those archiving device one may consider DVD burners, tape devices or transportable disks or whatever else that will be appropriate at the time of installation.

#### 6.16.2.6 Resource requirements

We have made estimates for the costs of the construction of three MX beamlines, see Tab. [A.1.3](#) for details. Expenses for construction of insulated hutches have not been accounted for. The estimates for the optical and vacuum components, X-ray detector, end-station and computer environment are based on the currently available quotes. We estimate that 9 person-years of a technical position and 3 person-years of a scientists position are required to construct each of the MX beamlines.

### 6.16.3 Biological small-angle X-ray scattering

**Authors:** M.V. Petoukhov and D.I. Svergun

**External advisors:**

Peter Boesecke	ESRF, Grenoble, France
Tetsuro Fujisawa	RIKEN, SPring-8, Himeji, Japan
Guenter Grossmann	SRS, Daresbury Laboratory, Daresbury, UK
Tom Irving	BioCAT, Illinois Institute of Technology, Chicago, USA
Javier Perez	Synchrotron Soleil, Gif-sur-Yvette, France
Ritva Serimaa	University of Helsinki, Finland
Hiro Tsuruta	SSRL, Stanford University, USA
Maria Antoinetta Vanoni	University of Milan, Italy
Regine Willumeit	GKSS Research Center, Geesthacht, Germany

#### 6.16.3.1 Introduction

During the last decade, small-angle X-ray scattering (SAXS) has become an increasingly important tool for the study of biological macromolecules. The method allows one to study native particles, from individual proteins to large macromolecular complexes, in solution under nearly physiological conditions. SAXS not only provides low resolution models of particle shapes but in many cases answers important functional questions. In particular, kinetic SAXS experiments allow one to analyze structural changes in response to variations in external conditions, protein-protein and protein-ligand interactions, and to effectively study equilibrium and non-equilibrium processes like assembly/dissociation of (macro)molecular complexes or folding/unfolding. Fundamental biological processes such as cell-cycle control, signalling, DNA duplication, gene expression and regulation, some metabolic pathways, depend on supra-molecular assemblies, and their changes over time. There are objective difficulties to study such complex systems, especially their dynamic changes by other structural techniques like spectroscopy, NMR and macromolecular X-ray crystallography (MX). Furthermore, for macromolecules with molecular masses of a few hundred kDa - too large for NMR and too small for cryo-electron microscopy (EM) - SAXS remains effectively the only method to obtain their shape in solution. Current trends in the life sciences point to a phase of integrated systems biology, which aims to understand living systems across the different levels of biological organization. Here, SAXS together with cryo-EM will provide the framework for the analysis of complex structures in which the high resolution models from MX and NMR can meaningfully be fitted.

The recent resurgence in biological SAXS is attributed to the synergy of software and hardware development. New powerful data analysis methods have become available ([Svergun & Koch, 2002](#)), which tremendously improved resolution and reliability of models deduced from SAXS data, and the new possibilities have significantly enlarged the user community. Simultaneously, SAXS instruments have been built on high brilliance 3<sup>rd</sup> generation synchrotron sources ([Irving, 1998](#); [Fujisawa et al., 2000](#); [Narayanan, Diat & Boesecke, 2001](#)). As the SAXS pattern is collected in the vicinity of the primary beam, the data quality depends critically on the beam size and divergence. SAXS is therefore among the techniques

which profit most from the low emittance undulator radiation on 3<sup>rd</sup> generation sources. Furthermore, the high flux of these sources is extremely important for the analysis of weakly scattering biological samples. Currently, high quality scattering patterns can be collected in less than a second using sub-mm beam sizes on the undulator SAXS beamlines like ID02 (ESRF, Grenoble, France), BL45A (SPring-8, Himeji, Japan), and BioCAT (APS, Argonne, USA).

The high brilliance undulator beamlines are revolutionizing biological SAXS in several ways. Firstly, they permit studies using limited amounts of material (sample volumes down to a few  $\mu\text{l}$  and solute concentrations below 1 mg/ml) thus significantly widening the range of applications. This advantage of the high brilliance sources is comparable to the use of small crystals in MX. Secondly, kinetic experiments to measure full solution scattering patterns in the millisecond range have recently become possible (e.g. [Schmolzer et al., 2002](#); [Akiyama et al., 2002](#); [Russell et al., 2002](#)). Moreover, the new sources will permit one to revive earlier and potentially powerful approaches like anomalous SAXS (ASAXS) for the analysis not only of counter ion distributions ([Guilleaume et al., 2002](#); [Das et al., 2003](#)) but also of bound biologically relevant metals and ions.

The parameters of the major present and planned SAXS beamlines partially used for life sciences on third generation sources are summarized in Tab. 6.16.2. None of these beamlines is dedicated to biological SAXS, except for BL45A at Spring-8, designed for high pressure and time-resolved experiments on solutions. The high flux beamline BL40XU (Spring8) utilizing pink beam is largely used for fluorescence and diffraction studies. The 8-ID IMM-CAT beamline at the APS, which permits coherent scattering studies with pink beam and time-resolved SAXS experiments, is largely devoted to material science. The 18-ID BioCAT beamline at the APS, designed for non-crystalline biological objects, is shared between three techniques (fiber diffraction, EXAFS and SAXS). The ID02 beamline at the ESRF optimized for the use at 0.1 nm wavelength in wide range of scattering vectors is primarily dedicated to soft condensed matter research. The ASAXS ID1 beamline yielding wide energy range is mostly used for materials research. The planned instruments at Soleil (France) and Diamond (UK) are multipurpose beamlines for research in the areas of condensed matter, materials and the life sciences.

### 6.16.3.2 Main features of the biological SAXS (BioSAXS) beamline

The present proposal aims at the construction of an undulator beamline for biological small-angle scattering at PETRA III. The main idea is to utilize the low emittance of the PETRA III source and the high brilliance of undulator radiation for providing the user community with a beamline, where the combination of the hardware and data analysis software opens the possibilities for high throughput (HTP) experiments and for cutting-edge research. This beamline will be built in the framework of the general EMBL concept for structural biology at PETRA III, but will also provide options for non-biological studies. The main features of the BioSAXS beamline are:

- The beam quality provided by the PETRA III undulator will be fully exploited to obtain a stable beam of high flux, small size and divergence yielding scattering patterns in the resolution range from about 2000 to 0.1 nm.

- The beamline will be tunable over a broad energy range allowing for ASAXS experiments on biologically relevant atoms or ions, from Ca to Mo (K-edges 4.038 and 19.99 keV, respectively). A high flux mode utilizing a multilayer monochromator is envisaged for the analysis of fast kinetics.
- A pink beam option will be provided for sub-ms kinetic studies, coherent scattering and pilot experiments for future XFEL applications.
- The beamline will share the infrastructure for biological sample preparation and handling with other planned EMBL beamlines and endstations. A pipeline will be envisaged to rapidly analyze proteins and protein complexes purified for the HTP crystallization facility.
- The sample environment will provide possibilities for performing HTP measurements with minimum amounts of material and for kinetic studies. An option will be included to collect crystallographic diffraction patterns from macromolecular assemblies with large unit cells.
- A data acquisition and analysis system will be installed at the beamline for automated data processing and interpretation allowing in particular large scale studies of biological macromolecules and three-dimensional model building.

### 6.16.3.3 Expected user community and collaborations

The construction of the proposed BioSAXS beamline responds to the rapidly increasing number of biological systems being studied and amenable to SAXS. EMBL runs the SAXS beamline X33 at DORIS III, and the number of biological projects at this beamline has grown annually by about 20% during the last four years. The BioSAXS beamline, combining excellent beam properties provided by PETRA III with the expertise in methods and automated data analysis developed at the EMBL, will make SAXS one of the major methods for the analysis of biological macromolecules. The current user community of the X33 beamline is expected to grow further, and the samples for the solution scattering analysis will come not only from individual research projects but also from systematic HTP protein production facilities.

A SAXS beamline with the proposed parameters (dynamic range, flux and beam size/divergence) will also be useful for soft condensed matter and material science applications (analysis of polymers, colloids and micro-emulsions, liquid crystalline phases, nanomaterials, fiber diffraction studies). Although the main priority of the BioSAXS beamline will lie in biological applications, the short measurement times and automation of the data processing/analysis will leave about 25% beamtime also for non-biological experiments. As a competent partner in this field, GKSS Research Center (Geesthacht, Germany) expressed interest in participating in the construction and operation of this beamline in collaboration with EMBL.

Instrument	Application	Monochromator	Mirrors (H)oriz / (V)ert. Focussing	E range, keV	Source-sample, m	Sample-detector, m	Flux	Spot, mm <sup>2</sup>	Divergence, $\mu$ rad <sup>2</sup>
<b>Operational beamlines</b>									
BL45A	SAXS	2×flat diamond (111) DCM	KB, V+H Rh coated	6.6-16	56	0.5-10	$1 \times 10^{13}$ @12keV	0.6×0.4	80×30
SPring-8	High flux	none, $\Delta\lambda/\lambda=2.0 \times 10^{-2}$	KB, V+H Si, Rh coated	8-17	48	0.5-4.5	$1 \times 10^{15}$ @12keV	0.25×0.04	Not given
8-ID, ANL	Coherent, time resolved SAXS	none(for pink beam) $\Delta\lambda/\lambda=2.6 \times 10^{-2}$	Flat Si, No focussing (slits)	7.7	55	4.5	$3 \times 10^{12}$	0.05×0.05	56×25
18-ID ANL	SAXS, EXAFS, Fiber	2×Si(111) or 2×Si (400) DCM (Flat + sagittally bent)	V: ULE/Pd/Pt coated	3.4-34	63	0.5-5.5	1-2×10 <sup>13</sup> @12keV	0.15×0.04	190×160
ID-02 ESRF	SAXS / USAXS	Si (111)	Toroidal coated	8-17	56	0.5 – 10	$5 \times 10^{13}$ @12keV	0.6×0.2	70×25
ID1 ESRF	ASAXS	2×Si (111), 2×Si(311) (Flat + sagittally bent)	V: Si/Rh/Pt Rh coated	2.1-42	46.1	0.5 – 5.0	$4.4 \times 10^{13}$ @8keV	0.2×0.06	500×70
<b>Projected beamlines</b>									
Beamline 11 Diamond	NCD ("life + physics")	Flat/bent crystal Si(111) or multilayer	Focussing mirror (+microfocus)	4-20 ( $\Delta\lambda/\lambda = 10^{-4}$ )	49	0.5-10	$5 \times 10^{12}$	0.10×0.01 (normal) 0.02×0.02 (micro)	200×20
SWING Soleil	SAXS / WAXS ("bio + soft")	Flat crystal 2×Si (or Ge)	KB V+H Pd - Si/Pd	5-15 ( $\Delta\lambda/\lambda = 10^{-4}$ )	32	0.5-10	$3 \times 10^{12}$	0.40×0.13	~75×20

Table 6.16.2: Parameters of SAXS beamlines used for life sciences on 3<sup>rd</sup> generation sources.

## 6.16.3.4 Instrument design

## Overall scheme and implantation

It is proposed to build the BioSAXS beamline on the second 2 m undulator U2 of a split straight section. The first 2 m undulator of this section will be used by the HTP EMBL MX beamline (ES2) and the users of the two beamlines (as well as of the XAS experimental station) will have direct access to the HTP crystallization facility (Fig. 6.16.9). The optical beam path of the MX beamline will be lifted by 30 cm by a double crystal monochromator (DCM), which will be positioned in the first ES2 optical hutch. The optical elements of the BioSAXS beamline will be positioned inside the optics hutch at a distance 35–47 m from the source, and the beam path will be diverted down and to the right to allow for sufficient separation from the ES2 beam pipe (Fig. 6.16.10A). The vacuum tube with the focused SAXS beam will pass through the second optical hutch of ES2 and its experimental hutch (47–60 m), and the SAXS user room (60–65 m). The experimental hutch of BioSAXS will occupy the space at 65–75 m.

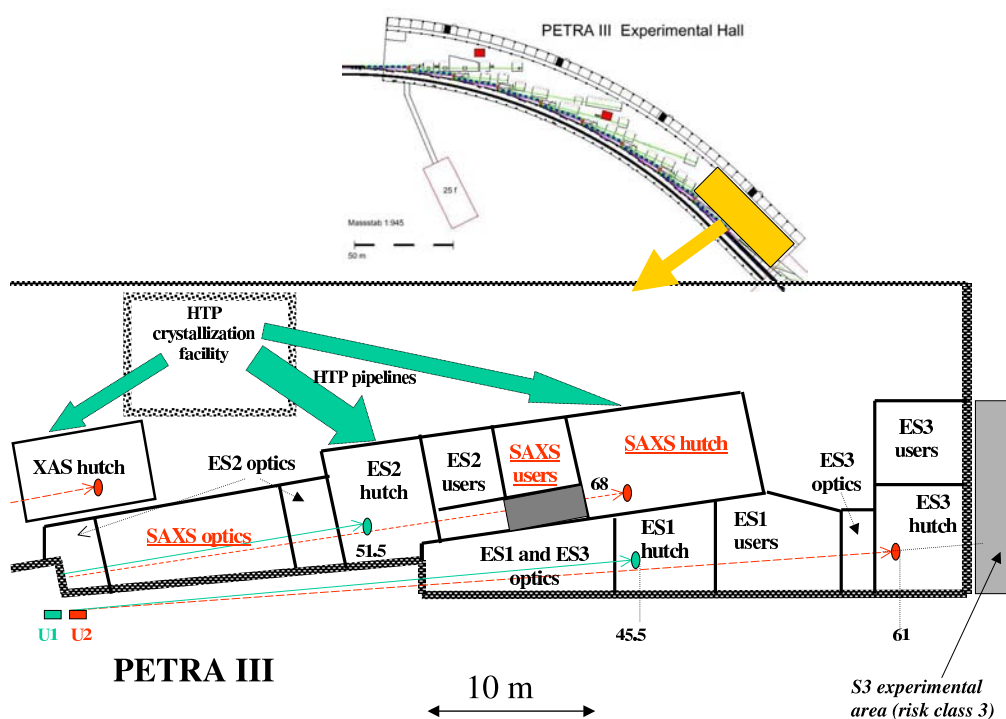


Figure 6.16.9: Overall scheme of the EMBL structural biology area with BioSAXS beamline components in red. Top: implantation of the EMBL area into the PETRA III experimental hall.

### Optical elements

Several possible options have been considered for the BioSAXS optics setup to optimize the beam size/divergence, stability and convenience of use. It was decided to use a flexible setup separating monochromatizing and focussing elements and to employ a moderately focussing configuration with small demagnification to minimize the beam divergence at the focus. Given the extremely low emittance of the PETRA III undulator, such a setup permits one to obtain a clean low divergence beam and to reach the scattering vectors corresponding to more than 2000 nm resolution.

The major elements of the beamline presented in Tab. A.1.5 and Fig. 6.16.10 are:

1. **Beryllium window and pinhole.** To reduce the absorption at low energies, a beryllium window of reduced thickness ( $250\ \mu\text{m}$ ) is proposed (at 4 keV, this window yields transmission  $T=67\%$  vs  $T=44\%$  of a  $500\ \mu\text{m}$  window). The position of the undulator beam will be detected by white beam monitors WBM (tungsten wire scan and/or slit scan, the latter detecting also the central cone). A cooled slit system (P) with variable size will select the most intense portion of the white beam thus reducing the heat load onto the subsequent optical elements.
2. **Monochromators.** A flat cryogenically cooled Si(111) fixed exit DCM is positioned at 37 m distance. We suggest the DCM to be the first optical element as it is relatively easy to adjust and monitor its position and orientation in the white beam by observing the Bragg reflection from the first crystal. The DCM will provide  $\Delta\lambda/\lambda=1-2\times 10^{-4}$  for possible ASAXS applications in the relevant energy range (from 4 to 20 keV). For high flux studies, the DCM will be replaced by a cryogenically cooled Mo/C double multilayer monochromator (MLM) at a distance of 38 m yielding two orders of magnitude gain in flux at the expenses of a broader bandpath (from  $\Delta\lambda/\lambda=1.5\times 10^{-2}$  at 7 keV to  $\Delta\lambda/\lambda=2.0\times 10^{-2}$  at 15 keV). Due to the smaller incidence angle of the MLM, the distance between the two multilayers will be larger than that between the crystals in the DCM (up to 0.7 m).
3. **Slits and beam monitoring.** Three pairs of cylindrical horizontal and vertical slits will be used (Fig. 6.16.10). Slit S1 will select the central cone of the undulator and define the beam size. Slit S2, located at about 5 m before the sample, will reduce the background from the optical elements, and the guard slit S3 in front of the sample will reduce the parasitic scattering from S2. The position of the monochromatic beam will be monitored by the removable fluorescent screens and pin diodes (beam monitors, BM). The intensity of the incoming beam will be measured by a removable pin diode and/or by a non-removable device like ionization chamber or glassy carbon placed after S3 in front of the sample and the transmitted intensity by the diode mounted onto the beam stop.
4. **Focussing mirrors.** A pair of cylindrically bent mirrors in Kirkpatrick-Baez (KB) configuration will be used for harmonics rejection and focussing (Fig. 6.16.10). The

first vertically focussing mirror (VFM1), positioned at 40 m, slightly reduces the vertical beam size (1:1.2 demagnification). The horizontally focussing mirror (HFM) at 45 m will reduce the horizontal beam size (1:1.6 demagnification). When used with the DCM and MLM, the water-cooled mirrors will work at a fixed incidence angle ( $0.18^\circ$ ) and fixed curvatures (11.5 km for VFM1 and 11 km for HFM) to focus the beam at 73 m. Each mirror will have two coatings (Si and Rh) to work in the energy ranges 4-9 keV and 9-20 keV, respectively (Fig. 6.16.11A).

5. **Pink beam mode.** For extra high flux (three times more than for MLM) and coherent scattering applications, a pink beam option will be provided with  $\Delta\lambda/\lambda=2\times 10^{-2}$ . This mode will be used for the energies around 8 keV, near the maximum brilliance of the fundamental undulator line. In this mode DCM and MLM will be removed from the optical path, and the first optical element will be a vertically focussing nitrogen cooled mirror VFM2 at 43.2 m (1:1.4 demagnification). This Si coated mirror will have the same focal point and grazing angle as VFM1 to keep the beam trajectory unchanged, so that there will be no need to adjust the focussing of the HFM.

The above configuration will ensure easy and rapid change of mode of operation between the DCM, MLM and pink beam options. The mirror inclinations will be fixed in normal modes of operation but could be changed if additional focussing elements like beryllium lenses will be introduced. All the optical elements will be positioned in the SAXS optical hutch to work under ultra-high vacuum conditions. Differential pumping will be employed to ensure that this portion of the beamline operates in ultra-high vacuum.

### 6.16.3.5 Beamline performance

To estimate the beam size, divergence and flux on the sample in the proposed configuration, ray tracing calculations were performed. The parameters of the 2 m long U2 PETRA III undulator were: period 2.9 cm,  $K_{max}=2.2$ , yielding the source size  $330\times 13\ \mu\text{m}^2$  and divergence  $26\times 21\ \mu\text{rad}^2$  (both horizontal $\times$ vertical FWHM). The simulations were done using the programs XOP (ESRF) and SHADOW (University of Wisconsin) for the three modes of operation: (i) DCM in the range 4-20 keV; (ii) MLM @ 8 keV; (iii) pink beam @ 8 keV. The position of the focus was at 73 m from the source, and the offset of the beam center with respect to the initial beam direction at the focus point was 17.6 cm (horizontal) and -18.7 cm (vertical) (Fig. 6.16.10A). All the computations were made for the partial flux through the aperture of  $1.2\times 0.7\ \text{mm}^2$  (horizontal $\times$ vertical) at 35 m distance (the pinhole size corresponding to the central cone). A  $0.5\ \mu\text{rad}$  mean slope error of the mirrors was assumed; mirror surface roughness up to 1 nm did not change the size and divergence significantly.

The beam size and divergence obtained by the ray tracing are presented in Fig. 6.16.10B,C. The materials, positions and orientations of optical elements are given in Tab. A.1.5 and the computed properties of the beam in Tab. 6.16.4. Fig. 6.16.11B presents the energy distributions in the partial flux for the configurations with DCM, MLM and pink beam. From comparison with the existing and planned SAXS beamlines on 3<sup>rd</sup> generation sources (Tab. 6.16.2) it can be concluded that the BioSAXS beamline will provide the overall widest

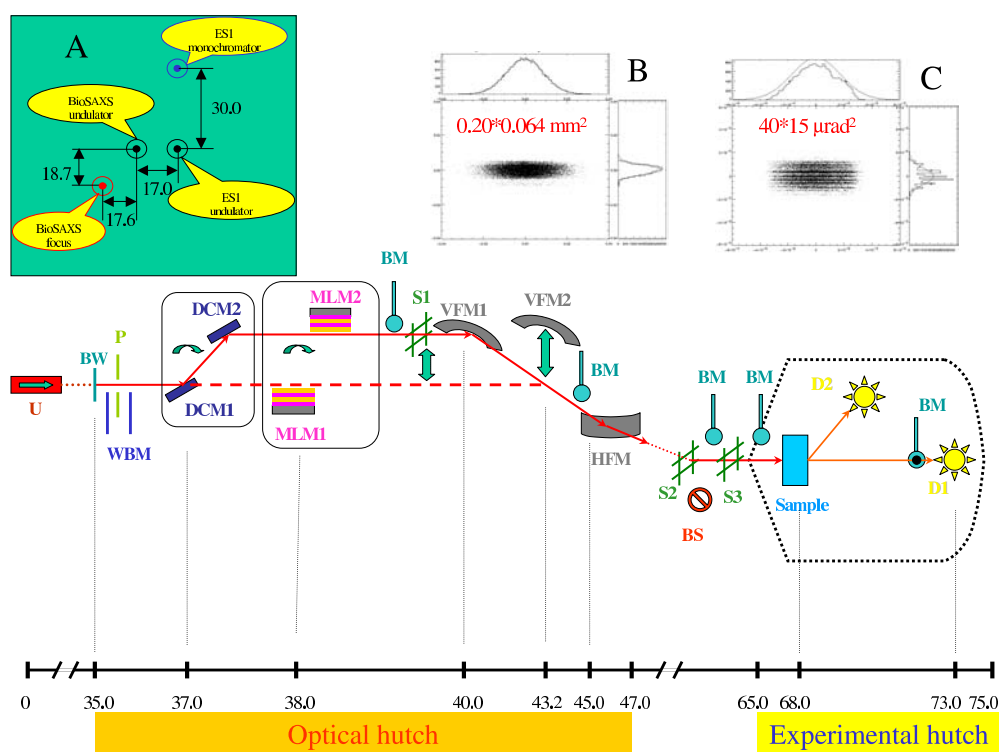


Figure 6.16.10: Schematic design of the BioSAXS beamline. The bottom scale displays distance from the source in meters; for explanations, see text. Insert A displays the cross section perpendicular to the beam direction at the focal point at 73 m from the source (distances are shown in cm). Inserts B and C present spatial and angular distribution of rays at the focal point simulated by SHADOW for a DCM setup at 8 keV.

experimental flexibility simultaneously yielding, thanks to the unique properties of the PETRA III beam, the best divergence for the given beam size.

Allowing for a beamstop size five times larger than the beam size (FWHM), the first useful experimental point in the vertical direction could be measured at about 0.3 mm. For a sample-detector distance of 5 m and the wavelength  $\lambda=0.15$  nm ( $E=8$  keV), this yields the minimum scattering vector  $s_{min}=2.5 \times 10^{-3}$  nm where  $s = (4\pi/\lambda)\sin(\theta)$ ,  $2\theta$  being the scattering angle. This yields the resolution up to  $d=2\pi/s_{min}=2500$  nm, comparable with that provided by USAXS (Ultra Small Angle X-ray Scattering) in Bonse-Hart geometry. This resolution of the setup is also justified by the ultra-small beam divergence at the sample: over a 5 m sample-detector distance, the effect of beam deterioration (smearing) due to the divergence does not exceed 0.1 mm.

If required for future applications (e.g. for observation of a few particle scattering from flash-frozen samples) the beam size could be further reduced (i.e. with beryllium lenses) at the expenses of divergence. The space for positioning the microfocussing lenses will be

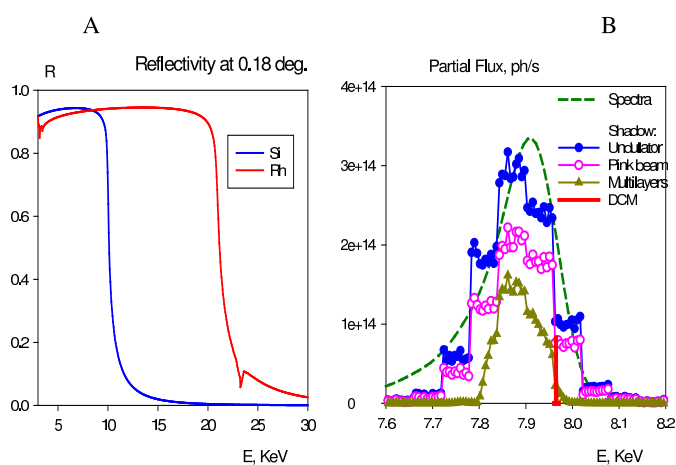


Figure 6.16.11: Reflectivity of the Si and Rh mirrors at the grazing angle of 0.18 degrees as a function of photon energy (A) and the partial flux (in 0.1%BW) of the U2 undulator at 8 KeV through a  $2.0 \times 1.5 \text{ mm}^2$  slit at 73 m calculated by SPECTRA (broken line), together with appropriately scaled SHADOW histograms of energy distribution in the beam using different monochromatization options.

available in the small hutch adjacent to the SAXS user room (gray shaded in Fig. 6.16.9; 60–65 m from the source).

### 6.16.3.6 Experimental hutch

The experimental hutch will have dimensions  $10 \times 5 \text{ m}^2$ . A motorized table (with a platform of  $1 \times 1 \text{ m}^2$  size able to accommodate pre-mounted sample holders of different types) will be positioned between the slits S3 and the entrance of the evacuated detector tube. A second copy of the table platform will be available for mounting another type of sample holder during the current experiment. The sample environment will contain the following options:

- thermostated automated changer of vacuum-tight cells for HTP studies
- thermostated setup with sample circulation to diminish radiation damage
- thermostated stopped-flow apparatus for fast kinetic studies
- cryo-cell to measure flash-frozen samples
- high pressure cell
- a coherent scattering spectrometer
- a triple axis goniometer for measuring crystals with large unit cells.

In most configurations, the sample will be kept in vacuum so that the detector tube will be connected to the vacuum tube containing the optical elements. This will allow to avoid extra windows and to minimize the background scattering and will also be useful for anaerobic experiments. Configurations to measure liquid and solid samples in open sample containers in air will be foreseen as well. A mechanical shutter (MS) will be installed between slits S2 and S3 for fast time resolved experiments.

The beam alignment at the sample position will be monitored by a position sensitive ionization chamber. Two detectors will be used to register the scattering at small and wide angles, whenever possible, simultaneously (SAXS and WAXS detectors D1 and D2, respectively). The sample-detector distances will be variable (SAXS detector: from 1 to 6 m, WAXS detector: 0.3 to 1 m). Off-center positions of the detectors will be foreseen to cover wider angular range, which requires a large diameter (about 1.0 m) detector tank (displayed in dashed line in Fig. 6.16.10). The SAXS detector will provide high count rates at low noise and cover wide dynamic ranges without spatial distortions. It is expected that the further development of hybrid pixel detectors (Berar et al., 2002) will lead by 2007 to the detectors of sufficient size to be effectively used for SAXS data registration. Another option would be e.g. a flat panel solid state selenium detector (MAR Research), which could also be employed for data collection at wide angles.

The user room ( $3 \times 5 \text{ m}^2$ ) will be placed before the experimental hutch for monitoring the experiment, on-site sample preparation and mounting. In addition to the acquisition system interface, the room will contain minimum sample storage and handling equipment like refrigerator, balance, centrifuge, etc. For specialized biochemical work the users may use the EMBL on-site facilities. Two offices for four persons (personnel, users) will be required in the office block of PETRA III.

### 6.16.3.7 Data analysis system

As the present beamline is designed for HTP studies, adequate real-time data processing and model-building techniques are indispensable. An integrated software system covering all the analysis steps from data reduction to automated modelling methods will therefore be installed at the beamline. It could be run either interactively via a menu-driven graphical user interface launching the data analysis modules or automatically for which a decision-taking block will be included to select proper analysis actions and to compare concurrent models. This system will be primarily oriented towards the analysis of biological macromolecules, but could also be used for non-biological isotropic and partially oriented objects (inorganic, colloidal solutions, polymers in solution and bulk).

The major components of the system will be:

- **Primary data processing and reduction package** based on the recently developed program package PRIMUS (Konarev et al., 2003) will employ standard data storage formats like Nexus (Maddison, Swofford & Maddison, 1997) and sasCIF (Malfois & Svergun, 2000). Major data processing steps will be performed automatically to compute characteristic functions and overall structural parameters.

Mode/property	Size (H), mm	Div. (H), $\mu\text{rad}$	Size (V), mm	Div. (V), $\mu\text{rad}$	Flux, ph/s
DCM 4 keV	0.21	43	0.061	20	$1.2 \times 10^{13}$
DCM 8 keV	0.20	40	0.064	15	$2.1 \times 10^{13}$
DCM 12 keV	0.21	38	0.067	10	$1.6 \times 10^{13}$
DCM 20 keV	0.21	35	0.066	10	$0.7 \times 10^{13}$
MLM 7.9 keV	0.21	45	0.060	26	$3.0 \times 10^{15}$
Pink 7.9 keV	0.21	45	0.051	28	$9.0 \times 10^{15}$

Table 6.16.4: Beam properties at the focal point calculated by SHADOW. Fluxes are computed accounting for transmission of a  $250 \mu\text{m}$  beryllium window.

- **Ab initio three-dimensional modelling suite** containing advanced and further developed *ab initio* programs (Svergun, 1999; Svergun, Petoukhov & Koch, 2001), will utilize the accurate scattering patterns in wide angular range (which can be reliably collected on the high brilliance BioSAXS beamline) to build macromolecular models with resolution to 1-0.5 nm. In large scale studies, these methods will be used to characterize proteins, which could not be crystallized at the HTP crystallization facility.
- **Rapid classification of proteins** will be performed using a database of scattering patterns computed from known high-resolution structures available in the Brookhaven Protein Data Bank (PDB). The prototype of the database is currently being developed (Sokolova, Volkov & Svergun, 2003)). Links to Web-based fold prediction sites will be provided with subsequent screening of the predicted models against the scattering data and against the *ab initio* models.
- **Addition of missing fragments and rigid body modelling** will be employed to further characterize proteins and protein complexes solved at high resolution using the HTP crystallographic pipeline. The recently developed methods (Petoukhov et al., 2002; Konarev, Petoukhov & Svergun, 2001) will be further developed and amended for the automated generation of structural models in large scale studies. Additional information from other methods (e.g. XAS data for metal-containing proteins) will be incorporated.
- **Quantitative analysis of interacting systems and mixtures** will be done using parametric linear least squares and non-linear fitting procedures and singular value decomposition (Konarev et al., 2003; Svergun et al., 2000) for time-resolved and titration experiments in the studies of processes like assembly, protein crystallization and (un)folding, as well as in the analysis of non-biological systems.

A functional prototype of the analysis system will be developed by 2007 and tested at the

EMBL beamline X33 at DORIS. It is planned to incorporate a training block into the system employing neural networks for advanced decision-taking and possible user-less operation.

#### 6.16.3.8 Conclusions

The proposed BioSAXS beamline will adequately exploit the exceptionally high brilliance of the PETRA III source to provide an experimental SAXS station with excellent parameters (dynamic range, flux and beam size, divergence) and broad capabilities. The BioSAXS beamline, linked to a HTP protein crystallization facility and equipped with a comprehensive data analysis system will comprise a unique environment for large scale SAXS analysis of biological macromolecules, and, in particular, for simultaneous MX/SAXS/XAS analysis. The beamline will also be available for soft condensed matter and material science applications. The construction of this beamline will further improve the efficiency of structural analysis using the small-angle scattering technique, and the expertise gained at BioSAXS will be shared with other large scale facilities in Europe and worldwide.

#### 6.16.3.9 Cost estimates

The total investment costs of the BioSAXS beamline is estimated to **2.7 M€**.

**Personnel** (minimum requirement assuming efficient support structure): 4 staff×3 years, 60 k€/person/year **0.7 M€**

**Total construction costs: 3.4 M€**

**Running costs:** 4×staff + maintenance: **about 0.5 M€/Year**